

Experimental and statistical analysis of carbon fiber/epoxy composites interleaved with nylon 6,6 nonwoven fabric interlayers

Journal of Composite Materials
2020, Vol. 54(27) 4173–4184
© The Author(s) 2020
Article reuse guidelines:
sagepub.com/journals-permissions
DOI: 10.1177/0021998320927740
journals.sagepub.com/home/jcm



Bertan Beylergil¹ , Metin Tanoğlu²  and Engin Aktaş³ 

Abstract

Thermoplastic interleaving is a promising technique to improve delamination resistance of laminated composites. In this study, plain-weave carbon fiber/epoxy composites were interleaved with nylon 6,6 nonwoven fabrics with an areal weight density of 17 gsm. The carbon fiber/epoxy composite laminates with/without nylon 6,6 nonwoven fabric interlayers were manufactured by VARTM technique. Double cantilever beam fracture toughness tests were carried out on the prepared composite test specimens in accordance with ASTM 5528 standard. The experimental test data were statistically analyzed by two-parameter Weibull distribution. The results showed that the initiation and propagation fracture toughness Mode-I fracture toughness of carbon fiber/epoxy composites could be improved by about 34 and 156% (corresponding to a reliability level of 0.50) with the incorporation of nylon 6,6 interlayers in the interlaminar region, respectively. The results also revealed that the percent increase in the propagation fracture toughness value was 67 and 41% at reliability levels of 0.90 and 0.95, respectively.

Keywords

Fracture toughness, thermoplastic interleaving, nylon 6,6, carbon fiber epoxy composites, Weibull distribution, statistical analysis

Introduction

Carbon fiber/epoxy (CF/EP) composites have been found in many engineering applications since they offer significant weight reduction and better corrosion and fatigue resistance compared to their metal counterparts. Delamination is the most dominant failure mode observed in these materials which promotes damage growth and premature failure. Therefore, researchers have devoted significant attention to searching techniques for improving delamination resistance of these materials.^{1–4}

Recently, interleaving technique based on insertion of an interleaf material at the interlaminar region has been developed. Various interleaf materials such as thermoplastic and thermoset films, nonwoven fabrics (micro or nano) and self-same resin interleaf materials can be used for improving interlaminar fracture toughness (IFT) of laminated composites. In this technique, interleaf material does not increase uncured resin viscosity and veil fibers are almost uniformly distributed in

the resulting laminate as compared to filler toughening.^{5,6} The following paragraph summarizes some of the recent studies on the effects of microfiber interleaving on the mechanical properties of different types of laminated composites.

Saz-Orozco et al.⁷ investigated the effects of polyamide (PA) and polyethylene terephthalate (PET) veils on the IFT of a glass fiber/vinyl ester (GF/VE) composites. The authors showed that PET veils have

¹Mechanical Engineering Department, Alanya Alaaddin Keykubat University, Turkey

²Department of Mechanical Engineering, Faculty of Engineering, Izmir Institute of Technology, Turkey

³Department of Civil Engineering, Faculty of Engineering, Izmir Institute of Technology, Turkey

Corresponding author:

Bertan Beylergil, Alanya Alaaddin Keykubat University Kestel Mah. Konya Cimento Ave. No: 80 Alanya, 07425 Turkey.
Email: bertan.beylergil@alanya.edu.tr

no significant effect on the IFT of composites while PA veils increased the mode I IFT values at crack initiation and propagation levels improved by 59% and 90%, respectively. Nash et al.⁸ and O'Donovan et al.⁹ also showed that IFT of CF/benzoxazine (BE) and GF/polyester (PE) composites could be increased by 352% and 170%, respectively. Fitzmaurice et al.¹⁰ also showed that PET veils were not effective for improving Mode-I IFT of the GF/PE composites due to the weaker glass/resin interface providing an alternative crack propagation path. It was shown that the incorporation of PET veils had positive effects on the flexural strength, interlaminar shear strength and damping properties of the composites. Kuwata¹¹ showed that PE nonwovens had the potential to improve IFT of CF/EP composites by 83%. Miller et al.¹² showed 40% increase in G_{Ic} with the addition of polyurethane (PU) veil. Ni et al.¹³ investigated the effects of aramid nonwoven fabrics on the mechanical properties of CF/bismaleimide (BMI) composites. Mode I IFT (G_{Ic}), Mode II IFT (G_{IIc}) and interlaminar shear strength of CF/BMI composites were also improved by 38.6%, 15.5% and 10.2%, respectively, with the incorporation of aramid nonwoven veils. Ramirez et al.¹⁴ investigated the effects of polyether ether ketone (PEEK) and polyphenylene sulfide (PPS) interleaf materials on the delamination resistance of CF/EP composites. The authors showed that PEEK and PPS were promising interleaf materials for improving fracture toughness of these composites significantly. Lee et al.¹⁵ investigated the effects of carbon nonwoven fabrics on the Mode-I fracture toughness under different temperatures. They concluded that the Mode-I fracture toughness was not significantly affected with the incorporation of carbon nonwoven fabrics under room temperature. Although few studies exist in the literature on the effects of nylon 6,6 microfibers on the IFT of laminated composites, further research is needed to clarify the effects of these microfibers on the IFT of laminated composites.

The Weibull distribution was firstly proposed by W. Weibull in 1939 and since then it has become one of the most important probability distributions for interpreting experimental data from various engineering fields and other science disciplines.¹⁶ Recently, Ono¹⁷ published a comprehensive review on the methods for simplifying estimation of the Weibull modulus. Due to the anisotropic behavior of composite materials, it is difficult to predict the mechanical properties of fiber reinforced composites accurately. Naresha et al.¹⁸ and Dirikolu et al.¹⁹ focused on the reliability analysis of tensile strengths of glass/epoxy (GF/EP) and carbon/epoxy (CF/EP) composites using Weibull distribution. Zhou et al.²⁰ carried out three-point bending tests on the neat CF/EP and MWCNTs reinforced

CF/EP composites and analyzed the test data using the two-parameter Weibull distribution. Fracture toughness of a composite material is not a deterministic property due to the stochastic nature of its microstructure. During the crack propagation, different fracture and/or toughening mechanisms are activated, and, thereby causing the scatter in fracture toughness.²¹ Therefore, it is important to employ statistical analyses for quantifying the fracture toughness of composites. To the best of the authors knowledge, this is the first study in which the effects of nylon 6,6 nonwoven fabrics on the IFT of CF/EP composites was statistically analyzed at different reliability levels.

In this study, nylon 6,6 microfibers were used as interleaf materials for improving delamination resistance of CF/EP composite laminates manufactured by VARTM technique. Double cantilever beam (DCB) tests were carried out on the reference and nylon 6,6 interleaved composites in accordance with ASTM 5528 standard. The Mode-I fracture toughness values were statistically analyzed by two-parameter Weibull distribution. The statistical results were presented at various reliability levels. Also, a comprehensive comparison of micro and nanofiber interleaving technique was made in the following sections.

Experimental

Manufacturing of CF/EP composite specimens

Plain woven carbon fabrics (with an areal weight density of 650 gsm (grams per square meter), Metyx Composites) were used as the primary reinforcement. The epoxy resin and its corresponding hardener (Momentive L160/H160, weight ratio: 80:20) were used as the matrix material. Commercial nylon 6,6 nonwoven fabrics (N-FusionTM) at an areal density of 17 gsm (thickness: 80 μ m) were provided by Cerex Advanced Fabrics Inc., USA. Scanning electron microscopy (SEM) observations were made to determine the morphology of the nylon 6,6 nonwoven fabrics. The specimens were sputter-coated with gold for 90 s and examined under a Philips XL 30 S FEG SEM. The SEM images of the nylon 6,6 nonwoven fabrics are shown in Figure 1. The average fiber diameter was determined as 20 μ m.

Differential scanning calorimetry (DSC) and thermal gravimetric analysis (TGA) were carried out to determine the degradation, melting and glass transition temperature of the nylon 6,6 nonwoven fabrics by Mettler Toledo TGA DSC + 3. Figure 2 shows the DSC and TGA curves of the nylon 6,6 nonwoven fabrics. In TGA analysis, the samples were heated from room temperature to 1000°C at a heating rate of 10°C/min under a nitrogen atmosphere. The degradation temperature

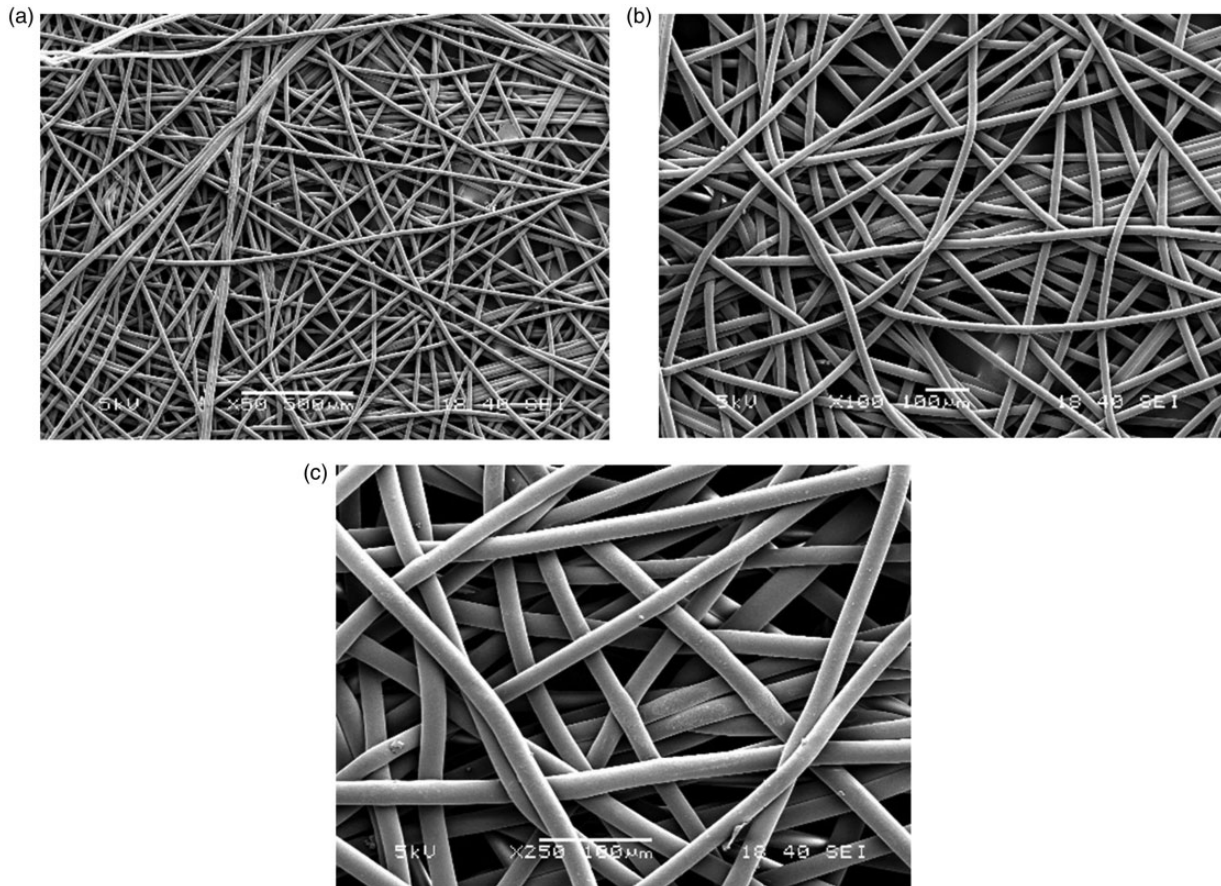


Figure 1. SEM images of nylon 6,6 microfibers at different magnification levels; (a) $\times 50$, (b) $\times 100$ and (c) $\times 250$. SEM: scanning electron microscopy.

was determined as 393.8°C . In DSC analysis, the samples were heated from room temperature to 350°C at a heating rate of $10^{\circ}\text{C}/\text{min}$ under a nitrogen atmosphere. The melting and glass transition temperature of the nylon 6,6 nonwoven fabrics were determined as 256.9°C and 87.3°C , respectively. DSC and TGA analyses clearly indicated that the PA 66 microfibers would retain their structure in the cured laminate since the curing temperature (80°C) was much lower than the melting and degradation temperature of the nylon 6,6 nonwoven fabrics.

The reference (eight woven carbon plies) and nylon 6,6 toughened (eight woven carbon plies + one nylon 6,6 nonwoven fabric) CF/EP composite laminates were produced by vacuum-infusion. Schematic representation of the lamination sequence of CF/EP composites with/without nylon 6,6 nonwoven fabrics is shown in Figure 3. The nylon 6,6 nonwoven fabric was only placed between the fourth and fifth plies to obtain minimal thickness change which directly affects the G_{IC} values. A non-adhesive film (Cytac Vac-Pak[®] A6200, thickness: $12\ \mu\text{m}$) was placed at the midplane of the laminate to act as a crack starter for the

delamination. The fabric stack was completely infused with the epoxy resin, then it was cured at room temperature followed by a proper post-curing at 80°C for 12 h as recommended by the manufacturer. The average thickness of the reference and nylon 6,6 interleaved composite specimens was determined as 5.11 mm. The reference and nylon 6,6 interleaved composite specimens were prepared by water jet cutting process. One of the longitudinal edges of the prepared composite specimens was painted white and marked for easier observation of the crack propagation.

Mode-I fracture toughness tests

The Mode-I IFT of the reference and nylon 6,6 interleaved composite specimens was determined by DCB testing in accordance with ASTM 5528.²² For each group, at least five specimens were tested as recommended in the standard. Schematic representation of the DCB test specimens is shown in Figure 4.

The DCB experiments were carried out by using a Shimadzu AGS-X universal test machine fitted with a 1-kN load cell. Each specimen was loaded with a

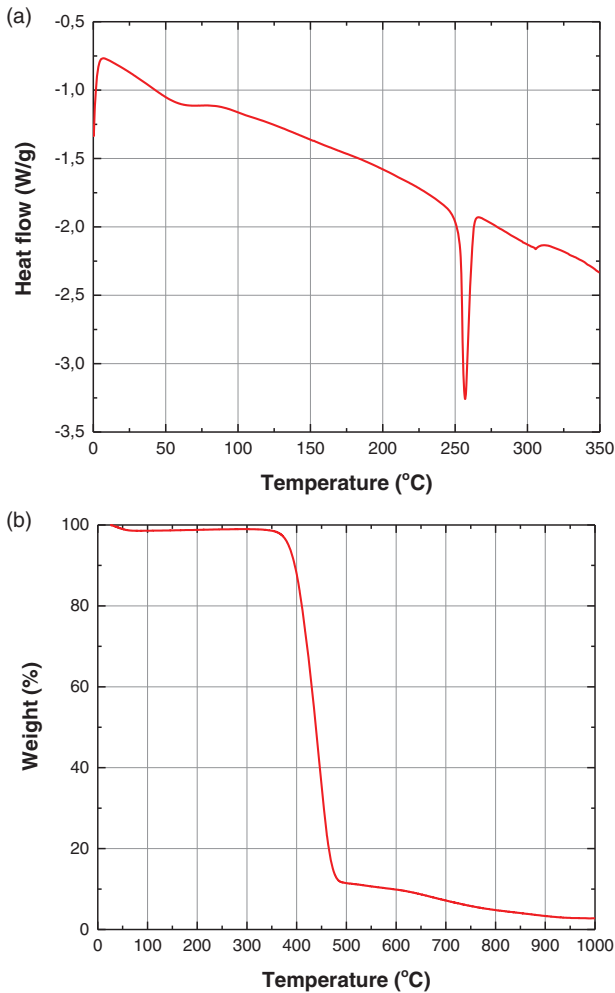


Figure 2. (a) DSC and (b) TGA curves of the nylon 6,6 non-woven fabrics.
DSC: differential scanning calorimetry; TGA: thermal gravimetric analysis.

crosshead speed of 1 mm/min until the delamination crack propagated along the full length of specimen. During the tests, the delamination growth was observed with a magnifying glass. For each crack jump, the load, opening displacement and crack length values were noted during the tests. G_I was calculated by using Modified Beam Theory given below²²

$$G_I = \frac{F}{N} \frac{3P\delta}{2b(a + |\Delta|)} \quad (1)$$

where P , δ , b and a are the applied load, opening displacement, width and delamination length, respectively. Δ is determined by generating a least squares plot of the cube root of compliance ($C^{1/3}$) as a function of delamination length. F and N are the correction parameters; the former accounts for tilting of the aluminum blocks whereas the latter considers the stiffening of the specimen by the blocks. These correction parameters can be determined by using the equations given below²²

$$F = 1 - \left(\frac{3}{10}\right) \left(\frac{\delta}{a}\right)^2 - \left(\frac{3}{2}\right) \left(\frac{\delta t}{a^2}\right) \quad (2)$$

$$N = 1 - \left(\frac{L'}{a}\right)^3 - \left(\frac{9}{8}\right) \left[1 - \left(\frac{L'}{a}\right)^2\right] \left(\frac{\delta t}{a^2}\right) - \frac{9}{35} \left(\frac{\delta}{a}\right)^2 \quad (3)$$

where the dimensions of t and L' are also illustrated in Figure 4. The initiation fracture toughness ($G_{Ic, ini}$) value was determined as the value of G_{Ic} at which the delamination was visually observed on the edge of the specimen. The fracture toughness during the steady-state crack propagation ($G_{Ic, prop}$) value was

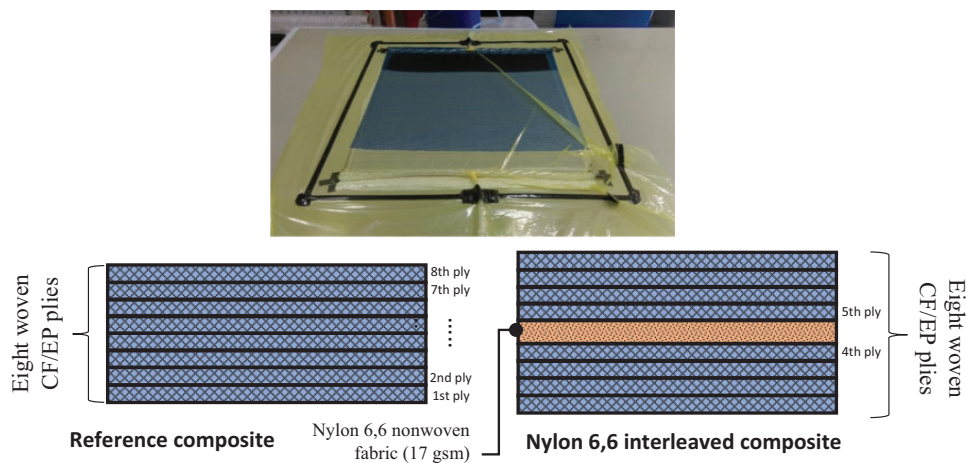


Figure 3. Vacuum infusion setup and schematic representation of lamination sequence of the woven composites.

calculated as the average of the G_{Ic} values during crack propagation.

Statistical analysis

In this study, the two-parameter Weibull distribution was used in the analysis of experimental data from fracture toughness tests. The density function, cumulative distribution function and reliability are given in equations (4) to (6), respectively. Here, $F(x)$ represents the probability that the fracture toughness is equal or less than x and $R(x)$, the reliability is the probability that the fracture toughness is at least x^{16}

$$f(x; \alpha, \beta) = \left(\frac{\beta}{\alpha}\right) \left(\frac{x}{\alpha}\right)^{\beta-1} \left\{ \exp\left(-\frac{x}{\alpha}\right)^\beta \right\}, x > 0, \alpha > 0, \beta > 0 \tag{4}$$

$$F(x) = 1 - \left\{ \exp\left(-\frac{x}{\alpha}\right)^\beta \right\} \tag{5}$$

$$R(x) = \left\{ \exp\left(-\frac{x}{\alpha}\right)^\beta \right\} \tag{6}$$

where α and β are the scale and shape parameters, respectively. These parameters were determined by using median rank regression method. In this method, a simple algorithm is used. First, the experimental data are sorted in ascending order and $x(i)$ denotes the i th smallest observation. Benard’s approximation (equation (7)) was used to estimate the median rank of $x(i)$. The term of $1-F(x)$ twice-logged (equation (8)) and the linear regression based on least squares minimization

was applied to the paired (X, Y) values (equation (9)), the scale and shape parameters were obtained²³

$$\widehat{f}(x(i); \alpha, \beta) = \frac{i - 0.3}{n + 0.4} \tag{7}$$

$$\ln \left[\ln \left(\frac{1}{1 - \widehat{f}(x(i); \alpha, \beta)} \right) \right] = \alpha \ln(x) - \alpha \ln(\beta) \tag{8}$$

$$(X, Y) = \left(\ln(x(i)), \ln \left[\ln \left(\frac{1}{1 - \widehat{f}(x(i), \alpha, \beta)} \right) \right] \right) \tag{9}$$

Results and discussion

Experimental and statistical results

Figure 5 shows the load-displacement curves of the reference and nylon 6,6 interleaved composite test specimens. The force increased with increasing displacement until it reached a maximum value then the force decreased as the crack jumps ahead in the interlaminar region. With increasing displacement, as the crack grows, a zig-zag pattern was obtained in the load-displacement curves of the composite specimens.

The average maximum force of the reference and nylon 6,6 interleaved composite specimens were determined as 83.5 ± 3.0 N and 138.8 ± 9.3 N, respectively. The average maximum force of the nylon 6,6 interleaved composites was 66.2% higher than that of the reference composites. The average maximum displacement of the reference and nylon 6,6 interleaved

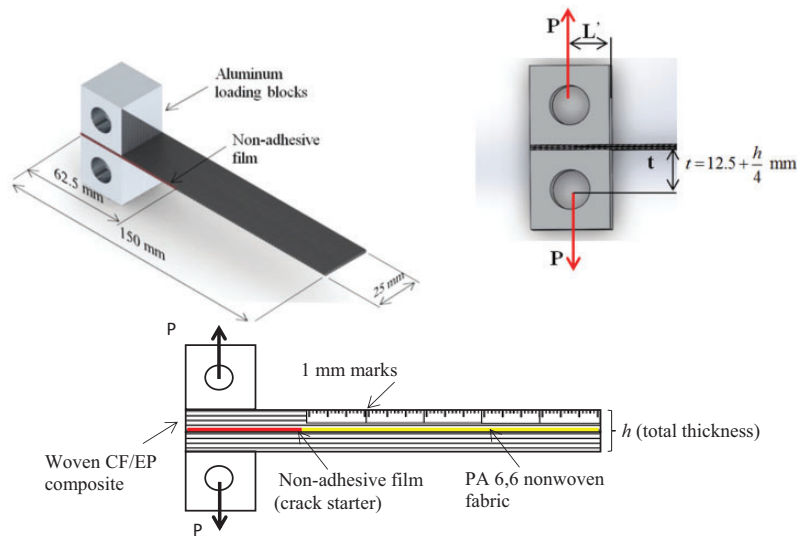


Figure 4. Schematic representation of the DCB test specimens. DCB: double cantilever beam.

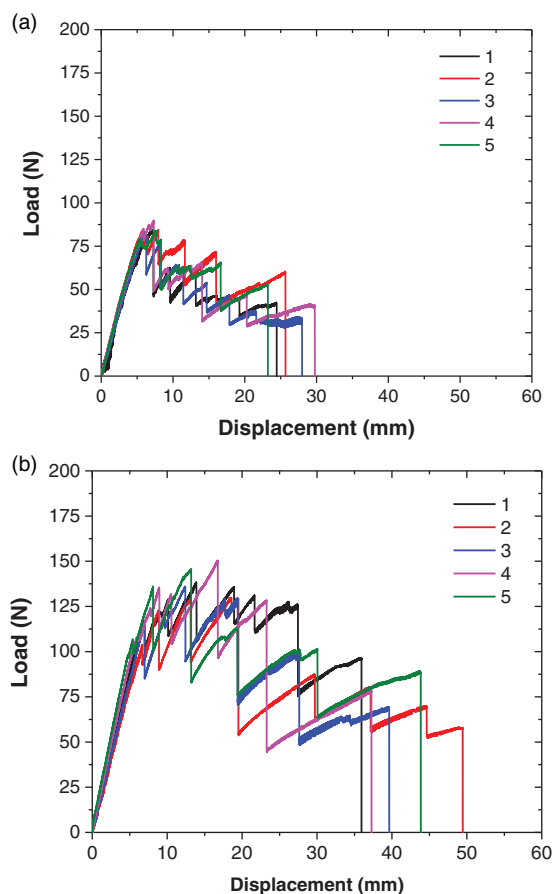


Figure 5. Load-displacement curves of the (a) reference and (b) nylon 6,6 interleaved composite specimens.

composite specimens were determined as 23.8 ± 3.3 and 37.3 ± 6.9 mm, respectively. The average maximum displacement of the nylon 6,6 interleaved composites was about 57% higher than that of the reference composites. The enormous increase in the force and displacement values can be attributed to that the microfiber bridging connects the two crack tips in the delaminated region of nylon 6,6 interleaved composites. The delamination crack interacted with thousands of randomly oriented/inclined nylon 6,6 microfibers in the interlaminar region and resulting in microfiber bridging. As the crack grew in the delaminated region, more energy was required to break the nylon 6,6 microfibers. Figure 6 shows least squares plot of the cube root of compliance ($C^{1/3}$) versus delamination length of the reference and nylon 6,6 interleaved woven composites.

Figure 7 shows the Mode-I fracture toughness (G_{Ic}) versus delamination length (a) curves, in other words the resistance curves of the reference and nylon 6,6 interleaved composite specimens. As can be seen in Figure 7(a), the reference woven composites had a characteristic resistance curve with a zig-zag pattern. The G_{Ic} values increase/decrease as the crack propagated.

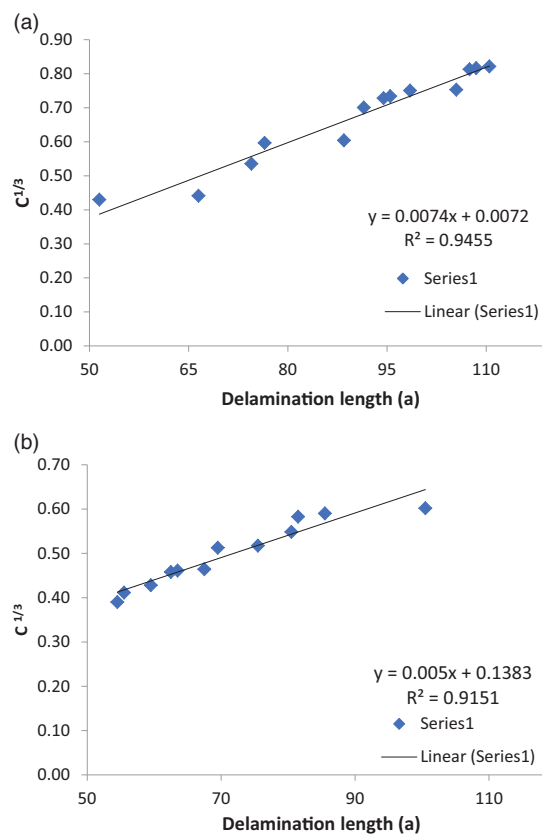


Figure 6. Least squares plot of the cube root of compliance, $C^{1/3}$, as a function of delamination length (a) reference and (b) nylon 6,6 interleaved composites.

This is due to the unstable crack propagation in woven composites. Figure 7(b) shows the resistance curve of the nylon 6,6 microfiber interleaved composites. The nylon 6,6 interleaved composites specimens showed different behavior as compared to the reference composites. The G_{Ic} values showed an increasing trend with increasing delamination length at the beginning of DCB experiments. This increasing trend is one of the main characteristics of the extensive fiber bridging which will be discussed later.²⁴ However, a small decrease in the fracture toughness values was observed after the crack propagated about 25 mm. The reason for this decrease can be explained in Figure 8 schematically. In the reference composite specimens, the crack propagated in the weak fiber/matrix interface, which resulted in lower fracture toughness values. On the other hand, in the nylon 6,6 interleaved composites, the crack jumped to the nylon 6,6 interlayer and propagated in this layer. Therefore, the steady-state crack propagation fracture toughness values increased as the crack continued to propagate in this layer. In this period, an extensive fiber bridging occurred which could be observed with naked eyes (please see side view of the nylon 6,6 interleaved composite specimen

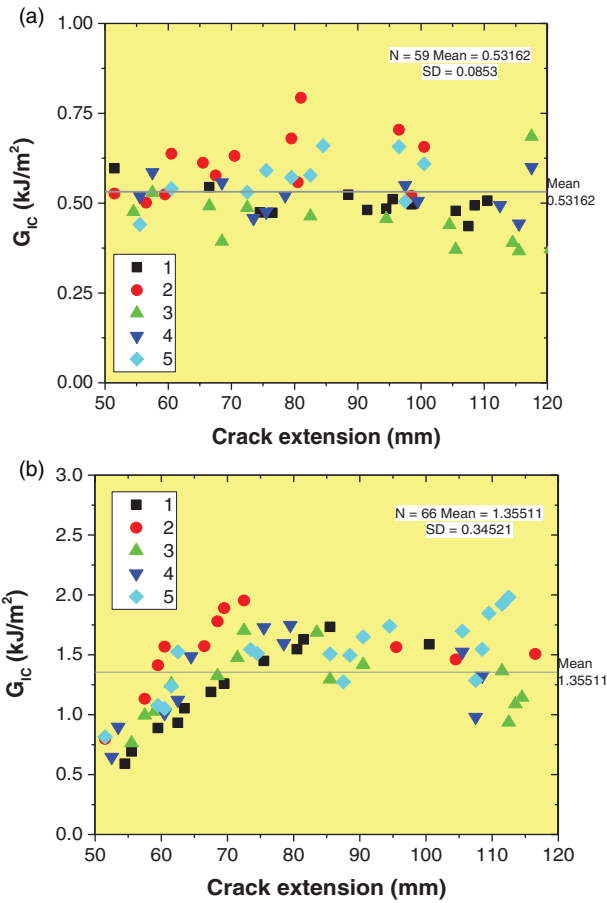


Figure 7. Resistance curves of the (a) reference and (b) nylon 6,6 interleaved composites.

shown in Figure 8) during the tests. The crack continued its journey in the nonwoven/nonwoven interface instead of carbon fiber/matrix interface. Once the crack encountered a relatively weak carbon fiber-epoxy matrix interface, the crack jumped to this interface, which resulted in a small decrease in steady-state fracture toughness values.

The average crack propagation fracture toughness values of reference and nylon 6,6 interleaved composites were determined as $0.531 \pm 0.08 \text{ kJ/m}^2$ and $1.345 \pm 0.14 \text{ kJ/m}^2$, respectively. The incorporation of nylon 6,6 interlayers in the interlaminar region led to significant increase of about 155.2% in the crack propagation fracture toughness values. The average maximum fracture toughness values of the reference and nylon 6,6 interleaved composites were determined as $0.66 \pm 0.08 \text{ kJ/m}^2$ and $1.82 \pm 0.13 \text{ kJ/m}^2$, respectively. This corresponds to 173.4% increase in the maximum fracture toughness values as compared to the reference composite specimens. The initiation fracture toughness of the reference and nylon 6,6 interleaved composites were calculated as 0.561 ± 0.05 and $0.752 \pm 0.118 \text{ kJ/m}^2$, respectively. The initiation fracture toughness increased

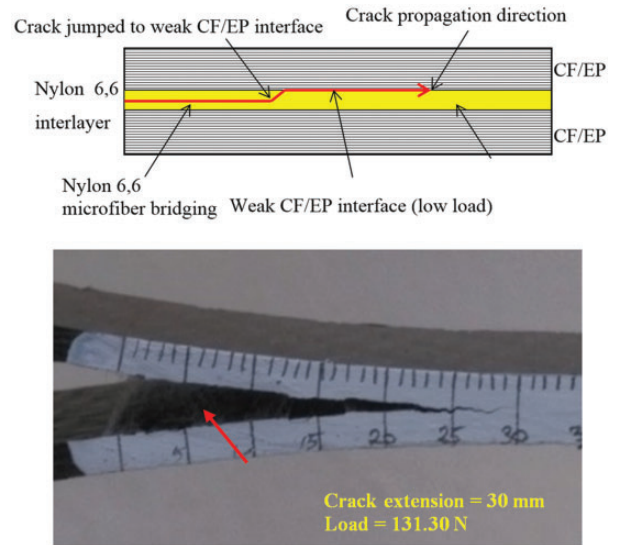


Figure 8. Schematic representation of the crack propagation and nylon 6,6 microfiber bridging observed in woven CF/EP composites. CF/EP: carbon fiber/epoxy.

by about 34% with the addition of nylon 6,6 nonwoven interleaf material as compared to reference specimens. It was also noteworthy that the standard deviation values of nylon 6,6 interleaved composites were higher (almost four times) than those of the reference composites. The crack jumps from fiber/matrix interface to interlayer and/or from interlayer to fiber/matrix interface during Mode-I loading. As a result, the fracture toughness data of nylon 6,6 interleaved composites deviated to a large extent from the average values showing a wider variation as compared to the reference composite specimens. Therefore, it can be said that it is required to conduct statistical analysis of the test data for the safe design of nylon 6,6 interleaved composites. Table 1 summarizes the experimental results of the reference and nylon 6,6 interleaved composite specimens under Mode-I loading.

Figure 9 shows the linear regression analysis results for reference and nylon 6,6 interleaved composites. Linear regression data statistics of reference and nylon 6,6 interleaved composites are shown in Table 2. The Weibull moduli of the reference and nylon 6,6 interleaved composites were determined as 7.28 and 4.34, respectively. The Weibull parameters α (scale) and β (shape) for reference and nylon 6,6 interleaved composites were determined as 0.56401 and 7.28725, 1.4895 and 4.3426, respectively. Due to the nylon 6,6 nonwoven interlayers, the scale parameter increased whereas the shape parameter decreased as compared to reference composites. This indicates the high fracture toughness scatter of interleaved composites. Figure 10 shows the G_{Ic} versus reliability ($R(x)$) plots for reference and nylon

Table 1. Mode-I fracture toughness test results.

	Specimen	Maximum force (N)	Maximum displacement (mm)	$G_{Ic,prop}$ (kJ/m ²)	$G_{Ic,max}$ (kJ/m ²)
Reference composites	I-1	84.62	22.96	0.504	0.597
	I-2	83.40	21.40	0.609	0.793
	I-3	83.22	24.68	0.456	0.685
	I-4	87.42	29.19	0.519	0.599
	I-5	79.02	21.09	0.568	0.659
	Average \pm SD	83.5 \pm 3.0	23.8 \pm 3.3	0.531 \pm 0.08	0.667 \pm 0.08
Nylon 6,6 interleaved composites	2-1	138.27	27.43	1.213	1.733
	2-2	129.82	44.49	1.505	1.953
	2-3	129.75	36.48	1.278	1.703
	2-4	150.47	34.86	1.278	1.747
	2-5	145.65	43.32	1.4838	1.982
	Average \pm SD	138.8 \pm 9.3	37.3 \pm 6.9	1.345 \pm 0.138	1.824 \pm 0.133

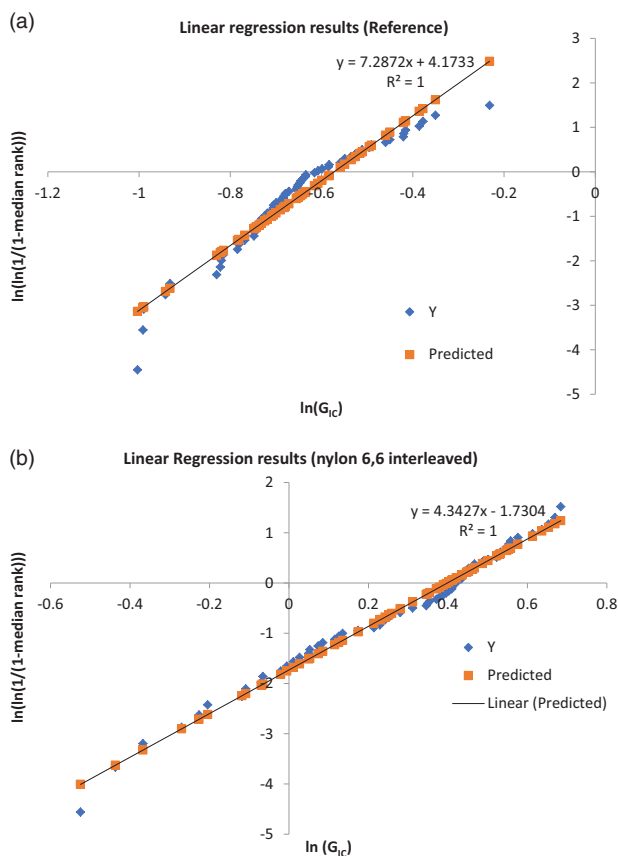


Figure 9. Linear regression results for (a) reference and (b) nylon 6,6 interleaved CF/EP composites. CF/EP: carbon fiber/epoxy.

6,6 interleaved CF/EP composites. As expected, fracture toughness values decreased with increasing reliability levels. This decrease was more pronounced in the nylon 6,6 interleaved CF/EP composites due to higher

standard deviations. It was noteworthy that the average steady-state crack propagation Mode-I fracture toughness value of nylon 6,6 interleaved composites approximately corresponded to a reliability level of 0.50. For reliability levels of 0.90 and 0.95, the steady-state crack propagation Mode I fracture toughness decreased from the average value of 1.345 kJ/m² to 0.887 kJ/m² and from 1.345 kJ/m² to 0.751 kJ/m², respectively. The percent increase in fracture toughness value due to nylon 6,6 nanofibers was determined as 67% and 41% at reliability levels of 0.90 and 0.95, respectively.

The comparison of the current study with the other results in the literature is shown in Table 3. The increase in IFT associated with different interleaf materials (at micro or nanoscale) and composite systems were reported. As can be seen, nylon 6,6 microfibrers are the most effective interleaf materials compared to the others. Our findings were shown to be consistent with the results reported in the literature. Another important observation was that the effectiveness of nonwoven interleaving system depends on the ability of fiber bridging of the microfibrers. CF and PET microfibrers remained inside of the epoxy matrix and they did not participate in fiber bridging mechanism during Mode-I loading. Therefore, only small improvements were obtained in fracture toughness values with the incorporation of these microfibrers in the interlaminar region of composites.

It can be also seen in Table 3 that there is a relationship between the number of microfibrers (in other words, areal weight density) and the fracture toughness. Interleaving heavy microfibrer nonwoven fabrics increases the effectiveness of the interleaf material; however, it deteriorates the other in-plane mechanical properties such as tensile, compressive and flexural properties.³¹ For instance, Beylergil et al.²⁵ studied

Table 2. Linear regression statistics.

	Observations (n)	Multiple-R	R ²	Adjusted R ²	Standard error
Reference composites	60	0.93677	0.87754	0.93546	0.31204
Nylon 6,6 interleaved composites	67	0.99405	0.98814	0.98796	0.13520

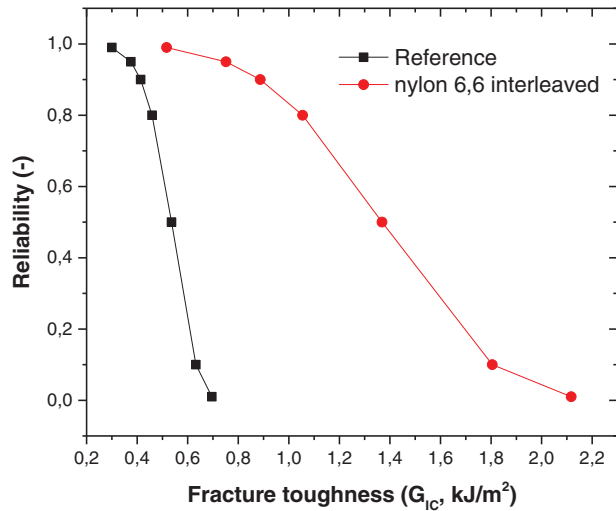


Figure 10. G_{IC} vs. reliability plots for reference and nylon 6,6 interleaved CF/EP composites. CF/EP: carbon fiber/epoxy.

the tensile and compressive properties of a carbon/epoxy [0°]₄ laminate interleaved with the 17 and 50 gsm nylon 6,6 nonwoven fabrics. They showed that the tensile and compressive strength decreased with improved areal weight density by about 41% and 13%, respectively. The trade-off between fracture toughness and in-plane mechanical properties can be minimized by doping some nanoparticles on interleaf material. A recent study by Quan et al.²⁶ showed that the performance of lightweight PPS could be increased significantly by doping different nanoparticles such as multi-walled carbon nanotubes (MWCNTs) and graphene nanoplatelets (GNPs) on the interleaf material. They stated that it was possible to improve Mode-I fracture toughness of CF/EP composites about 210% by using only 5-gsm PPS nonwoven fabric. Doping the thermoplastic interleaf material with GNPs and/or MWCNTs can be the solution for the reduced electrical conductivity which limits their usage in the aircraft structures.

Microfiber vs nanofiber interleaving

Table 3 shows the comparison of microfiber and nanofiber interleaving technique on the delamination resistance of laminated composites. Most of the studies focused on the nylon 6,6 nanofiber interleaving in the

Table 3. A comparison of the results of current study with the other micro/nano interleaving systems reported in the literature.

Reference	Composite system	Interleaf material	Areal weight density	% Increase in IFT
This study	CF/EP	m-nylon 6,6	17	155
7	GF/VE	m-nylon 6,6	17	90
8	CF/BE	m-nylon 6,6	34	352
9	GF/PE	m-nylon 6,6	17	170
10	GF/VE	m-PET	45	12
11	CF/EP	m-PE	20	83
12	GF/PE	m-PU	15	40
13	CF/BMI	m-AR	16	108
14	CF/EP	m-PEEK	11	102
14	CF/EP	m-PPS	40	133
15	CF/EP	m-CF	12	28
25	CF/EP	m-nylon 6,6	17	171
26	CF/EP	m-PPS-MWCNTs	5.0	210
26	CF/EP	m-PPS-GNPs	5.0	159
27	CF/EP	n-nylon 6,6	1.5	55
27	CF/EP	n-nylon 6,6	4.5	156
27	CF/EP	n-nylon 6,6	9.0	173
28	CF/EP	n-nylon 6,6	1.0	50
29	CF/EP	m-AR	8.5	72
30	CF/EP	m-PET	8.0	85
30	CF/EP	m-PPS	5.0	65

VE: vinyl ester; BE: Benzoxazine; m: micro; n: nano; PE: polyethylene; BMI: bismaleimide; PET: Polyethylene terephthalate; AR: aramid; PU: polyurethane; PEEK: Polyether ether ketone; PPS: Polyphenylene sulphide; MWCNTs: multi-walled carbon nanotubes; GNPs: graphene nanoplatelets.

literature. It is obvious that nylon 6,6 is the most promising material among the other polymers in terms of improvement in delamination resistance of laminated composites. It is noteworthy that nanofiber interleaving is more effective than microfiber interleaving. The delamination resistance of laminated composites could be improved significantly by using smaller number of nanofibers in the interlaminar region as compared to microfiber interleaving. For instance, it was shown that the incorporation of nylon 6,6 nanofibers with an areal density of 1.0 g/m² led to significant

increase in Mode-I fracture toughness values of CF/EP composites about 50%.

As in the case of microfiber interleaving, there is a relationship between the number of nanofibers in the interlaminar region and fracture toughness improvement. Beckermann and Pickering²⁷ showed that it was possible to improve fracture toughness about 55% by using PA nanofibers with an areal weight density of 1.5 g/m². The delamination resistance of composites was improved by 155% as the areal weight density was tripled. Then, the improvement in fracture toughness reached a plateau with the increase of nanofiber amount (9.0 g/m²) in the interlaminar region. As previously stated, although the microfiber interleaving improves Mode-I fracture toughness significantly, it deteriorates in-plane mechanical properties of composite laminates due to the reduced fiber volume fraction, thickness increase and formation of voids.²⁵ In nanofiber interleaving technique, it is possible to improve not only delamination resistance but also in-plane mechanical properties of composite laminates. This win-win situation is the unique characteristic of nanofiber interleaving technique. For instance, Molnar et al.³² showed that the incorporation of polyacrylonitrile (PAN) nanofibers could improve the interlaminar shear strength of unidirectional CF/EP composites by 11%. Also, they showed that the flexural strength and modulus of these composites could be increased by 21% and 54%, respectively. Charpy impact test results showed that the energy to maximum force could be increased by 64% by incorporating PAN nanofibers in the interlaminar region of CF/EP composites. It is noteworthy that the proper selection of polymer type is a critical issue considering the benefits provided in terms of mechanical performance.

The nanofiber interleaving technique can be considered the best solution for the delamination problem in the laminated composites. Technological developments in multi-nozzle electrospinning devices also makes this technique more promising. A fascinating example is the Nanospinner Industrial Electrospinning Line developed by Inovenso Inc., which has a nanofiber production capacity of 5 kg per day.³³ The nanofiber interleaving technique is evolving and can be used in engineering structures that are subjected to the out-of-plane loading in service and particularly prone to delamination. Instead of using in the whole structure, the critical areas such as near holes, notches and sharp corners, where the risk of delamination is high, can be locally interleaved with polymeric nanofibers.

The transition of the nanofiber-interleaving technique into commercial products has already started, and now the first commercial supplies of thermoplastic nano interlayers are on the market. However, there are some issues that should be considered before

commercialization step. For instance, the use of highly volatile and hazardous chemicals such as formic acid and chloroform is the critical issue that needs to be considered. Another critical issue is that the producing of electrospun nanofibers with uniform diameter and thickness since the diameter of nanofibers³⁴ and the thickness of nanointerlayers²⁷ were identified as two key factors that play the primary role in the success of nanofiber interleaving. To create electrospun nanofiber interlayers uniformly, the multiple-nozzle electrospinning process should be continued for a long period of time. During this period, the polymeric solution may solidify at one of the nozzle tips (clogging or blockage of the nozzles) which slow down or obstruct the electrospinning process. To fully startup the electrospinning device again, time-consuming procedures are required. Moreover, the clogging of the nozzles may cause the loss of stability. If the electrospinning process is unstable, the thickness and diameter of the nanofibers will not be uniform. The thickness/diameter variations in the nanofiber interlayers will cause significant increase in the standard deviations.

Concluding remarks

In this study, nylon 6,6 nonwoven fabrics were used as interleaf materials for improving Mode-I delamination resistance of CF/EP composite laminates manufactured by VARTM technique. DCB tests were carried out on the reference and nylon 6,6 interleaved composites in accordance with ASTM 5528 standard. The Mode-I fracture toughness values were statistically analyzed by two-parameter Weibull distribution. The experimental and statistical results were presented at different reliability levels. Summarizing the presented results, the following conclusions could be drawn:

- The initiation fracture toughness of CF/EP composites by about 34% using nylon 6,6 nonwoven fabrics in the interlaminar region.
- The crack propagation Mode-I fracture toughness of CF/EP composites could be increased by about 156% using nylon 6,6 nonwoven fabrics in the interlaminar region.
- The nylon 6,6 microfibers prevented the CF/EP plies from opening and slowed down the crack propagation in the interlaminar region. The main toughening mechanism was microfiber bridging between the adjacent plies of CF/EP composites.
- The steady-state crack propagation Mode-I fracture toughness value of nylon 6,6 interleaved composites corresponded to a reliability level of 0.50. The percent increase in fracture toughness value was 67% and 41% at reliability levels of 0.90 and 0.95, respectively.

- Weibull probabilistic method could be used for reliable and safe design of nylon 6,6 interleaved composite laminates.

Declaration of Conflicting Interests


The author(s) declared no potential conflicts of interest with respect to the research, authorship, and/or publication of this article.


Funding

The author(s) received no financial support for the research, authorship, and/or publication of this article.

ORCID iDs

Bertan Beylergil  <https://orcid.org/0000-0002-3204-6746>

Metin Tanoğlu  <https://orcid.org/0000-0001-9770-1302>

Engin Aktaş  <https://orcid.org/0000-0002-5706-2101>

References

- Greenhalgh ES, Rogers C and Robinson P. Fractographic observations on delamination growth and the subsequent migration through the laminate. *Compos Sci Technol* 2009; 69: 2345–2351.
- Greenhalgh ES. *Failure analysis and fractography of polymer composites*. Woodhead Publishing Series in Composites Science and Engineering, CRC Press, 2009, 164–165.
- Hojo M, Ando T, Tanaka M, et al. Modes I and II interlaminar fracture toughness and fatigue delamination of CF/epoxy laminates with self-same epoxy interleaf. *Int J Fatigue* 2006; 28: 1154–1165.
- Nakai Y and Hiwa C. Effects of loading frequency and environment on delamination fatigue crack growth of CFRP. *Int J Fatigue* 2002; 24: 161–70.
- Sela N and Ishai O. Interlaminar fracture toughness and toughening of laminated composite materials: A review. *Compos* 1989; 20: 423–435.
- Yasaee M, Bond IP, Trask RS, et al. Mode I interfacial toughening through discontinuous interleaves for damage suppression and control. *Compos A Appl S* 2012; 43: 198–207.
- Saz-Orozco BD, Ray D and Stanley WF. Effect of thermoplastic veils on interlaminar fracture Toughness of a Glass Fiber/Vinyl Ester Composite. *Poly Comp* 2017; 38: 2501–2508.
- Nash NH, Young TM and Stanley WF. The reversibility of Mode-I and -II interlaminar fracture toughness after hydrothermal aging of carbon/benzoxazine composites with a thermoplastic toughening interlayer. *Compos Struct* 2016; 152: 558–567.
- O'Donovan K, Ray KD and McCarthy MA. Toughening effects of interleaved nylon veils on glass fabric/low-styrene-emission unsaturated polyester resin composites. *J Appl Polym Sci* 2014; 132: 41462.
- Fitzmaurice K, Ray D and McCarthy MA. PET interleaving veils for improved fracture toughness of glass fibre/low-styrene-emission unsaturated polyester resin composites. *J Appl Polym Sci* 2016; 133: 42877.
- Kuwata M. *Mechanisms of interlaminar fracture toughness using non-woven veils as interleaf materials*. PhD Thesis, University of London, UK, 2010.
- Miller SG, Roberts G, Kohlman L, et al. Impact behavior of composite fan blade leading edge subcomponent with thermoplastic polyurethane interleave. In: *Proceedings of 20th international conference on composite materials*, Denmark, 19–24 July 2015, pp.1–12.
- Ni N, Wen Y, He D, et al. High damping and high stiffness CFRP composites with aramid non-woven fabric interlayers. *Compos Sci and Technol* 2015; 117: 92–99.
- Ramirez VA, Hogg PJ and Sampson WW. The influence of the nonwoven veil architectures on interlaminar fracture toughness of interleaved composites. *Compos Sci and Technol* 2015; 110: 103–110.
- Lee S-H, Noguchi H, Kim Y-B, et al. Effect of interleaved non-woven carbon tissue on interlaminar fracture toughness of laminated composites: Part II – Mode I. *J Compos Mater* 2002; 36: 2169–2181.
- Hallinan AJ. A review of the Weibull distribution. *J Qual Technol* 1993; 25: 85–93.
- Ono K. A Simple estimation method of Weibull modulus and verification with strength data. *Appl Sci* 2019; 9: 1575.
- Naresha K, Shankar K and Velmurugan R. Reliability analysis of tensile strengths using Weibull distribution in glass/epoxy and carbon/epoxy composites. *Compos B Eng* 2018; 133: 129–144.
- Dirikolu MH, Aktas A and Birgoren B. Statistical analysis of fracture strength of composite materials using Weibull distribution. *Turk J Eng Env Sci* 2002; 26: 45–48.
- Zhou Y, Pervin F, Lewis L, et al. Fabrication and characterization of carbon/epoxy composites mixed with multi-walled carbon nanotubes. *Mater Sci Eng A* 2008; 475: 157–165.
- Li Y and Zhou M. Prediction of fracture toughness scatter of composite materials. *Comp Mater Sci* 2016; 116: 44–51.
- ASTM D5528-13. *Standard test method for mode I interlaminar fracture toughness of unidirectional fiber-reinforced polymer matrix composites*. Annual book of ASTM standards, West Conshohocken, PA, 2013.
- Lysiak G. Fracture toughness of pea: Weibull analysis. *J Food Eng* 2007; 83: 436–443.
- Pokluda J and Šandera P. *Micromechanisms of fracture and fatigue: In a multi-scale context*. 1st ed. London: Springer, 2010.
- Beylergil B, Tanoğlu M and Aktaş E. Effect of polyamide-6, 6 (PA 66) nonwoven veils on the mechanical performance of carbon fiber/epoxy composites. *Compos Struct* 2018; 194: 21–35.
- Quan D, Mischo C, Binsfeld L, et al. Fracture behaviour of carbon fibre/epoxy composites interleaved by MWCNT- and graphene nanoplatelet-doped thermoplastic veils. *Compos Struct* 2020; 235: 105642.
- Beckermann G and Pickering K. Mode I and Mode II interlaminar fracture toughness of composite laminates interleaved with electrospun nanofibre veils. *Compos A Appl S* 2015; 72: 11–21.

28. Beylergil B, Tanoğlu M and Aktaş E. Enhancement of interlaminar fracture toughness of carbon-fiber epoxy composites using polyamide-6,6 electrospun nanofibers. *J Appl Polym Sci* 2017; 134: 45244.
29. Beylergil B, Tanoğlu M and Aktaş E. Mode-I fracture toughness of carbon fiber/epoxy composites interleaved by aramid nonwoven veils. *Steel Compos Struct* 2019; 31: 113–123.
30. Quan D, Bologna F, Scarselli G, et al. Interlaminar fracture toughness of aerospace-grade carbon fibre reinforced plastics interleaved with thermoplastic veils. *Compos A Appl S* 2020; 128: 105642.
31. García-Rodríguez SM, Costa J, Rankin KE, et al. Interleaving light veils to minimise the trade-off between mode-I interlaminar fracture toughness and in-plane properties. *Compos A Appl S* 2020; 128: 105659.
32. Molnar K, Kostakova E and Meszaros L. The effect of needleless nanofibrous interleaves on mechanical properties of carbon fabrics/epoxy laminates. *Express Polym Lett* 2014; 8: 62–72.
33. Nanospinner 416 Industrial Electrospinning Line; inovenso, <https://www.inovenso.com/portfolio-view/nanospinner416> (accessed 3 October 2020).
34. Zhang J, Lin T and Wang X. Electrospun nanofibre toughened carbon/epoxy composites: Effect of polyetherketone cardo (PEK-C) nanofibre diameter and interlayer thickness. *Compos Sci Technol* 2010; 70: 1660–1666.